EFFECT OF ROTATING CYLINDER ON THE DRAG FORCE OF A ROAD TRUCK VEHICLE

Najdat N. Abdulla
Prof.Dr./ University of Baghdad

Alaalddin A. Ismail
Mechanical Engineer

ABSTRACT

The effect on aerodynamic drag of a truck by controlling the boundary layer separation using a rotating cylinder on leading edge of the truck-trailer is investigated numerically. The flow was assumed to be steady, incompressible, turbulent, and two-dimensional passing over the top surface of the truck. The boundary condition for all the boundaries of the truck was set as well as the cylinder was treated as a moving wall with a specific rotational velocity. The developed computational algorithm is tested for the flow over a flat plate (8m) long with various free stream inlet relative velocity ($U\infty$) which are considered the same as truck velocity and has the values (40, 60, 90, and 120) km/h. The effect of cylinder diameter (10,20,30,and 40) , rotational speed (1000-5000 r.p.m) and free stream velocity on the aerodynamic drag and pressure distribution of the flow field were investigated. The governing equations which used are the continuity, momentum, and the (K-ε) turbulence model. These equations are approximated by using a finite volume method, with staggered grid and modified SIMPLE algorithm. A computer program in FORTRAN 90 is built to perform the numerical solution.The numerical results show that, the optimum cases for inlet free stream relative velocity ($U\infty$) values(40,60) km/h, a significant reduction of drag coefficient equal to 80% and 77% respectively was obtained by useing a speed of rotation and diameter size equal to 5000 r.p.m and 40 cm , for ($U\infty$) value(90)km/h a reduction equal to76%, and for ($U\infty$) equal to (120) km/h a reduction equal to 60% was obtained . These optimum results lade to reduce the effect of the aerodynamic drag on the vehicle by delaying the separation zone of boundary layer and enhancing the pressure gradient of the flow field. Comparison of the results with the available previous published experimental and fluent program results was investigated.

الخلاصة

تم بحث في التأثير على مقاومة حركة جريان الهواء على نموذج شاحنة بواسطة السيطرة على انفصال الطبقة المتاخمة عن طريق حقـن الزخم (momentum injection) باستعمال اسطوانة دوارة في الحافة العليا لمقدمة مقطورة الشاحنة بحثا عدديا،افترض الجريـان بأنـه مستقر غير انضغاطي غير مضطرب و كذلك ثنائي البعد ،يمر فوق السطح العلوي للشاحنة. جميع الظروف المتاخمة للـشاحنة تعامـل على أنها جدار ثابت عدا الاسطوانة الدوارة فأنها تعامل كجدار متحرك بسرعة دورا نية معينة. النموذج العددي يتضمن الجريـان علـى صفيحة مستوية طولها (8م) مع سرعة جريان داخلة متغيرة للسطح الحر ($U\infty$) و التي تمثل سرعة الشاحنة نفسها و قيمها (40، 60، 90، 120) كلم /ساعة.العملية تضمنت تغيير السرعة الدورانية و القطر للاسطوانة الدوارة مع كل مقدار من سرعة الجريان الحـر($U\infty$) لتوضيح تأثير الدوران على مقاومة حركة جريان الهواء و توزيع الضغط في حقل الجريان ، تم استخدام القطر بأبعاد (10 ، 20 ، 30 ، 40) سم مع سرعة دورا نية تتراوح بين (1000-5000) دورة بالدقيقة.المعـادلات الرياضـية الرئيـسية المـستخدمة هـي معـادلات الاستمرارية، الزخم، ومعادلة نموذج (K - ε) للاضطراب. تم حل المعادلات عدديا باستخدام طريقـة الحجـوم المحـددة (Finite Volume Method) مع الشبكة المزحفة (Staggered Grid) باستخدام خوارزميـة (Simple Algorithm) . تـم بنـاء برنـامج حاسوبي بلغة (FORTRAN 90) لانجاز الحل العددي.النتائج العددية أظهرت بحصول انحسار مميز لمعامل مقاومة حركـة جريـان الهواء و يختلف باختلاف سرعة جريان السطح الحر($U\infty$) وكانت النسبة المئوية للانحسار للسرع (60,40) كلم/سـاعة تـساوي 80%،

77% بالتتابع و ذلك بأستخدام سرعة دورانية بقيمة (4000) دورة بالدقيقة و قطر بقياس (30) سم ، و النسبة المئوية للانحسار للـسرعة (90) كلم/ساعة تساوي 76%،كذلك النسبة المئوية للانحسار للسرعة (120) كلم/ساعة تساوي 60% .هذه النتائج أدت إلى تقليـل تـأثير مقاومة جريان حركة الهواء عن طريق تأخير ظهور عملية انفصال الطبقة المتاخمة و تحسين انحدار الضغط في حقل الجريـان.عمليـة مقارنة نتائج البحث مع النتائج العملية المتوفرة والنتائج التي تم الحصول عليها باستخدام برنامج (fluent)أعطت نتائج متقاربة.

Keywords: boundary layer control, rotating cylinder, computational fluid dynamics, road vehicles.

INTRODUCTION

Boundary layer separation takes place under adverse pressure gradient conditions when viscous effects are no longer confined to a thin layer but affect the overall flow pattern drastically**, Singh (2005)**. It can be seen that an adverse pressure gradient, ($\partial p / \partial x > 0$), is a necessary condition for separation. It does not mean that if ($\partial p / \partial x > 0$), a separation will occur, but rather it is reasoned that separation cannot occurs unless ($\partial p / \partial x > 0$). The point on the boundary where $[\partial u / \partial y]_{y=0}$ =0 is called the point of separation. Just downstream from the point of separation, the flow direction in the separated region is actually opposite to the main flow direction. The low energy fluid in the separated region is forced back upstream by the increased pressure downstream **Robert (1973, 1978)**. The most common application to date has been the flow around an aerofoil wing of an aircraft. Flow separation takes place on the upper surface of the aerofoil at a large angle of attack resulting in a drastic fall in lift. Several methods, such as mass injection either by blowing or by suction, coating of the wall, or transition to turbulent flow etc. have been practiced with varying degrees of success. The concept of delaying boundary layer separation has also been used in road vehicles to reduce aerodynamic drag. However, the use of momentum injection using a moving wall for boundary layer control is still in its nascent stages. Momentum injection using rotating cylinders has been applied to airfoils in order to improve their lift characteristics like applied the concept of moving surface boundary layer control to a joukowsky airfoil using rotating cylinders at the leading and trailing edges of the airfoil. However, the use of rotating cylinders to reduce aerodynamic drag on tracks is a new concept **Singh (2005)**. At 70 mph, a common highway speed today, overcoming aerodynamic drag represents about 65% of total energy expenditure for a typical heavy truck vehicle. Reduced fuel consumption for heavy vehicles can be achieved by altering truck shapes to decrease the aerodynamic resistance or drag. It is conceivable that present day truck drag coefficients might be reduced by as much as 50%. This reduction in drag would represent approximately a 25% reduction in fuel use at highway speeds **Rose (2004)**.

Singh et.al {2005}, investigated aerodynamic drag effect using a model of a truck to control the boundary layer separation by the momentum injection method using a rotating cylinder. They used an experiments coupled with computational fluid dynamics (CFD) analysis to validate the theory of momentum injection. Modeling of the truck has been done on the software (GAMBIT); the best suitable turbulence model was selected by comparing the results with the experimental results. Steady state Navier Stokes equations are taken as the governing equations for the fluid motion, and appropriate boundary conditions are used. The rotational speed and radius of the cylinder are varied to establish the effect of momentum injection on aerodynamic drag. The coefficient of drag reduces by approximately 35 percent from an initial value of 0.51- 0.32 for a cylinder of radius 1cm with rotational speed of 4000 r/min. **Robson et.al {2005},** used a generic rotating ventilator as a form of low energy drag reducer for use on bluff bodies such as transport vehicles. An experimental investigation of a rectangular bluff body was conducted to demonstrate the viability of this novel concept. The ventilator is expected to produce an effect on the flow characteristics similar to a rotating cylinder but with the added advantage that it can be operated using natural wind without the need for any power input by the engine or any auxiliary unit. The bluff body was modeled as a rectangular box; the ventilator was mounted on the front of the model with the axis of rotation parallel to the front surface and bottom edge. Open circuit open jet wind tunnel was used to conduct the experiments. The test Reynolds numbers were selected to lie between $3.5 – 6.5 \times 10^5$,measurements were taken at yaw angles of 0, 5, 10, 15 degrees. The results indicate that the device decreases drag on the body significantly by approximately 50% at Reynolds numbers of 3.5×10^5 and 6.5×10^5 . The

incorporation of this device also makes the drag of the body less Reynolds number dependent. Consequently the proposed configuration is more efficient at higher speed in comparison with the conventional configuration which did not have the device attached to it.

Salam Al-Taee {2005}, studied the separation control on the ***NACA 0012 & NACA 0018*** airfoils by using a rotating cylinder based on the computation of Reynolds-average Navier-Stokes equations. A numerical model based on collocated finite volume method is developed to solve the governing equations on a body-fitted grid. To ensure the accuracy of the code first, second and third order differencing schemes, with and without flux-limiters, have been implemented and tested. The systematical investigation of the rotating cylinder is conducted on the same ***NACA 0012*** airfoil in the range of attack angles from 10^0 up and beyond the stall angle at $Re=10^6$ .the influence of some parameters associated with using rotating cylinder, such as its radius, location, and the speed ratio (U_C/U_∞) strength on the performance of the airfoils have been studied. The result shows that the rotating cylinder is affected in controlling the separation and the lift coefficient of circulation control airfoil is increased with the angle of attack. **Robert Clark {2006},** presented a combination of wind tunnel test, computational fluid dynamic modeling, and real-world testing to determine the effects of the external additions devices and systems on aerodynamic drag and fuel economy. These devices include (cab enclosure, vortex traps, side strakes, and side skirts). The results showed a reduction on the aerodynamic drag by 23% for tractor-semitrailer systems. **Johan Hoffman {2007},** considered the problem of computational simulation of flow past a wheel of a vehicle. As a model he used a rotating cylinder in contact with a flat surface moving with the same velocity as the uniform free stream. In particular he was interested in the importance of including the effect of rotation in the model to accurate compute the drag force. He compared two different models; (i) a cylinder rolling around ground, and (ii) a stationary cylinder in free stream, corresponding to a simple wind tunnel testing. He compared the drag for (i) and (ii) at Reynolds number of 10000. He used CFD method to investigate the importance of including (i)-(ii) in a model. As computational model he considered the flow about cylinder rolling along a flat surface. CFD concerns the computational solution of the Navier-Stokes equations, which are considered to model both laminar and turbulent flow. In this paper study the flow of turbulent boundary layer over a flat plate, study the effect of a rotating cylinder (in order to inject momentum) on the aerodynamic drag, utilizes CFD method and standard κ-ε model to analyze the effect of momentum injection on the aerodynamic drag, use different values of rotation speeds to demonstrate the effect of rotation on the drag coefficient and use different values of diameter size to demonstrate the effect of diameter size on the drag coefficient.

MATHEMATICAL MODEL

The starting point of any numerical method is the mathematical model, i.e. the set of partial differential or integral-differential equations and boundary conditions. These equations are based on the conservation of mass and momentum. A finite volume method (FVM) is presented for the solution of two-dimensional Navier-Stokes equations in a Cartesian coordinate. The (k-ε) model is utilized to describe the turbulent flow on the upper surface of the truck. The flow was assumed to be steady, two- dimensional and incompressible over a flat plate with a rotating cylinder in the leading edge of the plate.

Geometry and Coordinate System:

The usual system of Cartesian coordinates is adopted which represents the x-axis being along the wall and the y-axis being at right angle to it, as shown in **Fig. (a)** .

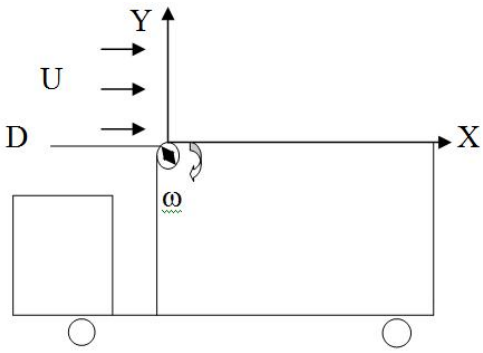

Figure.(a).

The Governing Equations:

The equations of motion for steady state, two dimensional and incompressible flows over flat plate can be written as follows ,**Robert(1973,1978)**:-

(i) Continuity Equation

$$\frac{\partial}{\partial x}(\rho u)+\frac{\partial}{\partial y}(\rho v)=0 \qquad (1)$$

(ii) Momentum Equations

X– Direction (u – momentum)

$$\frac{\partial}{\partial x}(\rho uu)+\frac{\partial}{\partial y}(\rho u\nu)= -\frac{\partial p}{\partial x}+\mu\left[\frac{\partial^2 u}{\partial x^2}+\frac{\partial^2 u}{\partial y^2}\right] \quad (2)$$

Y-Direction (ν- momentum)

$$\frac{\partial}{\partial x}(\rho u\nu)+\frac{\partial}{\partial y}(\rho\nu\nu)= -\frac{\partial p}{\partial y}+\mu\left[\frac{\partial^2 \nu}{\partial x^2}+\frac{\partial^2 \nu}{\partial y^2}\right] \quad (3)$$

The effects of fluctuation can be introduced by replacing the flow variable u, ν, ρ and p by the sum of mean and fluctuating components. Thus, Versteeg **(1995)**:

$$\left.\begin{aligned} u &= \overline{U}+u' \\ \nu &= \overline{V}+\nu' \\ P &= \overline{P}+p' \end{aligned}\right\} \quad (4)$$

With some simplification the momentum equations become, **Awbi(1991)**:

$$\rho U\frac{\partial U}{\partial x}+\rho V\frac{\partial U}{\partial y}=-\frac{\partial P}{\partial x}+\frac{\partial}{\partial x}\left[\mu_e\frac{\partial U}{\partial x}\right]+ \frac{\partial}{\partial y}\left[\mu_e\frac{\partial U}{\partial y}\right]+\frac{\partial}{\partial x}\left[\mu_e\frac{\partial U}{\partial x}\right]+\frac{\partial}{\partial y}\left[\mu_e\frac{\partial V}{\partial x}\right] \quad (5)$$

$$\rho U\frac{\partial V}{\partial x}+\rho V\frac{\partial V}{\partial y}=-\frac{\partial P}{\partial y}+\frac{\partial}{\partial x}\left[\mu_e\frac{\partial V}{\partial x}\right]+ \frac{\partial}{\partial y}\left[\mu_e\frac{\partial V}{\partial y}\right]+\frac{\partial}{\partial x}\left[\mu_e\frac{\partial U}{\partial y}\right]+\frac{\partial}{\partial y}\left[\mu_e\frac{\partial V}{\partial y}\right] \quad (6)$$

Turbulence Model:

Standard K-ε Model

The general modified form of (K-ε) model can be written as follows, **Versteeg (1995)**:

$$\rho U\frac{\partial K}{\partial x}+\rho V\frac{\partial K}{\partial y}=\frac{\partial}{\partial x}\left[\frac{\mu_t}{\sigma_k}\frac{\partial K}{\partial x}\right]+\frac{\partial}{\partial y}\left[\frac{\mu_t}{\sigma_k}\frac{\partial K}{\partial y}\right]+ \mu_t\left[2\left(\frac{\partial U}{\partial x}\right)^2+2\left(\frac{\partial V}{\partial y}\right)^2+\left(\frac{\partial U}{\partial y}+\frac{\partial V}{\partial x}\right)^2\right]-\rho\varepsilon \quad (7)$$

$$\rho U\frac{\partial \varepsilon}{\partial x}+\rho V\frac{\partial \varepsilon}{\partial y}=\frac{\partial}{\partial x}\left[\frac{\mu_t}{\sigma_\varepsilon}\frac{\partial \varepsilon}{\partial x}\right]+\frac{\partial}{\partial y}\left[\frac{\mu_t}{\sigma_\varepsilon}\frac{\partial \varepsilon}{\partial y}\right]+ c_{1\varepsilon}\frac{\varepsilon}{K}\mu_t\left[2\left(\frac{\partial U}{\partial x}\right)^2+2\left(\frac{\partial V}{\partial y}\right)^2+\left(\frac{\partial U}{\partial y}+\frac{\partial V}{\partial x}\right)^2\right]-c_{2\varepsilon}\rho\frac{\varepsilon^2}{K} \quad (8)$$

The empirical constants appearing in the above equation have the values of, **Fayadh (2004/2005)**:-

$\mathbf{C_\mu}$***=0.09*** $\mathbf{C_{1\varepsilon}}$***=1.44*** $\mathbf{C_{2\varepsilon}}$***=1.92*** $\boldsymbol{\sigma_K}$***=1.00*** $\boldsymbol{\sigma_\varepsilon}$***=1.3*** $\boldsymbol{\sigma}$***=0.7*** $\boldsymbol{\sigma_t}$***=0.9***

Further Calculation:

The most important parameters for boundary layer flow, is drag coefficient C_{Df}:

$Drag= 1/2\rho V^2 A\ C_{Df}$

Where $\boldsymbol{C_{Df}}$: coefficient of skin friction drag.
A: is the surface area.
ρ: is the density of the air.
V: is the speed of the vehicle relative to the air.

COMPUTATIONAL TECHNIQUE

The solution of the continuity and momentum equations was performed by using a finite volume method (FVM) to obtain the discretization form for these equations. These discretization equations are solved by using SIMPLE algorithm with hybrid scheme. A computer program based on this algorithm and uses FORTRAN 90 language was built to meet the requirements of the problem. The SIMPLE algorithm was based on the staggered grid in which the velocities staggered midway between the grid intersections is used to obtain the numerical results.

The General form of the Governing Equations, Versteeg (1995):

$$\frac{\partial}{\partial x}\left(\rho u\Phi\right)+\frac{\partial}{\partial y}\left[\rho v\Phi\right]= \frac{\partial}{\partial x}\left[\Gamma_\Phi\frac{\partial \Phi}{\partial x}\right]+\frac{\partial}{\partial y}\left[\Gamma_\Phi\frac{\partial \Phi}{\partial y}\right]+S_\Phi \quad (9)$$

Where Φ, Γ_Φ, S_Φ define in table (1) as flow

Table (1) Source terms in the transport equation.

Equation	ϕ	Γ_ϕ	S_ϕ
Continuity	1	0	0

U-momentum	U	μ_e	$-\frac{\partial P}{\partial x}+\frac{\partial}{\partial x}\left[\mu_e\frac{\partial U}{\partial x}\right]+\frac{\partial}{\partial y}\left[\mu_e\frac{\partial V}{\partial x}\right]$
V-momentum	V	μ_e	$-\frac{\partial P}{\partial y}+\frac{\partial}{\partial x}\left[\mu_e\frac{\partial U}{\partial y}\right]+\frac{\partial}{\partial y}\left[\mu_e\frac{\partial V}{\partial y}\right]$
Kinetic energy	K	Γ_K	G- ρε
Dissipation rate	ε	Γ_ε	$C_{1\varepsilon}\rho\frac{\varepsilon}{K}G-C_{2\varepsilon}\rho\frac{\varepsilon^2}{K}$

Where:

$$G=\mu_t\left[2\left(\frac{\partial U}{\partial x}\right)^2+2\left(\frac{\partial V}{\partial y}\right)^2+\left(\frac{\partial U}{\partial y}+\frac{\partial V}{\partial x}\right)^2\right] \quad (10)$$

$$\Gamma_k=\frac{\mu_e}{\sigma_K}\qquad \Gamma_\varepsilon=\frac{\mu_e}{\sigma_\varepsilon} \quad (11)$$

$$\Gamma_e=\frac{\mu}{\sigma}+\frac{\mu_t}{\sigma_t} \quad (12)$$

Grid Generation:

To avoid the instability in the solution, and unrealistic pressure field, the staggered grid technique has been adopted. Staggered grids imply that different dependent variables are evaluated at different grid points. The scalar variables are stored at the main grid points, while the velocity components are stored at staggered grids (the velocities are defined at the faces of control volumes). Hence, the scalar variables including pressure are stored at the main grid nodes denoted by small circles, **Versteeg (1995).**

Discretization of the general form of Equations:

The final discretised algebraic equation, **Versteeg (1995)**:

$$A_P\phi_P=A_E\phi_E+A_W\phi_W+A_N\phi_N+A_S\phi_S+S_u \quad (13)$$

Where:

$$A_p=A_E+A_W+A_N+A_S-S_p \quad (14)$$

$$\left.\begin{aligned}A_E&=D_e-\frac{F_e}{2}\\A_W&=D_w+\frac{F_w}{2}\\A_N&=D_n-\frac{F_n}{2}\\A_S&=D_s+\frac{F_s}{2}\end{aligned}\right\} \quad (15)$$

Were the above equations can be expressed in general form for different types of schemes as **Patankar (1980)**:

$$\left.\begin{aligned}A_E&=D_eA(|Pe|)_e+[[-F_e,0]]\\A_W&=D_wA(|Pe|)_w+[[F_w,0]]\\A_N&=D_nA(|Pe|)_n+[[-F_n,0]]\\A_S&=D_sA(|Pe|)_s+[[F_s,0]]\end{aligned}\right\} \quad (16)$$

Here, $A(|Pe|)$ is a function concerned with various types of schemes. Expressions for $A(|Pe|)$ for different schemes are listed in Table (4-2) in which |Pe| is peclet number $(Pe=\mathrm{Re}\,\mathrm{Pr})$ at the control volume faces which may be expressed as the ratio of the strength of convection term (F) to that of diffusion term (D). The operator [[A …]] appearing in equations refers to the maximum value of the quantities contained within it.

Table (2) Function A (|Pe|) for different schemes, Patankar (1980).

Scheme	Formula for A(|Pe|)
Central difference	1-0.5|Pe|
Upwind	1
Hybird	[[0,1-0.5|Pe|]]
Power law	[[0,(1-0.1|Pe|)^5]]
Exponential	|Pe|/[exp(|Pe|)-1]

RESULTS AND DISCUSSION

Fig. (1) Shows the effect of varying the mesh size on the drag coefficient at rotation speed ω=2000 and cylinder diameter D=40 cm. A grid independency test is preformed to check the validity of the numerical technique, the numbers of nodes which had been taken are (2800, 3200, 3600, 4000). It is clear that the influence of the mesh size on the drag coefficient was small, so (3200) nodes was selected for all calculations.

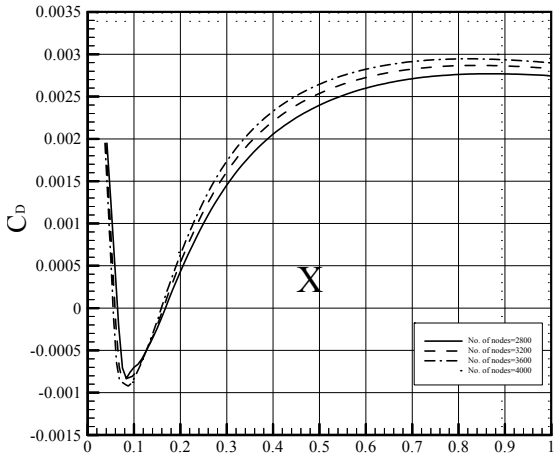

Figure. (1) Effect of mesh size on the drag coefficient.

The parameters that had a direct influence on the amount of reduction in the drag coefficient are the rotation speed (ω), and diameter size (D), thus the effect of each parameter was studied in separate cases according to the value of vehicle speed ($U\infty$) as will shown in the figures.

Fig. (2.a-d) show the effect of variation of cylinder rotation speeds on the drag coefficient (C_D) and wall shear stress (τ_w) with vehicle speed ($U\infty$) equal to 60 km/h. The cases are classifying according to diameter size. When the cylinder rotates, the fluid starts to inject over the surface, this action creates a low pressure zone directly after the cylinder and this causes an appearing of a streamwise vortices **Solberg (1989)**.This streamwise jet help the air flow to cling more closely to the upper surface {1}, and this is leading to delay the separation zone and reduce the drag coefficient. The amount of reduction depends on rotation speed as shown in the figures. For the case of D=10, 20 cm, it can be seen that the drag coefficient (C_D) increases along distance as the rotation speed increases, but for cases of D=30, and 40 cm the drag coefficient decreases as the rotation speed increases. For small cylinder diameter the momentum injected of the flow is small and will not create enough streamwise vortices to help the flow to cling closely to the surface which has a reverse influence on the flow.

Also, it can be seen in the figures that an extreme dropping in the drag coefficient, this due to the streamwise vortices zone and low pressure accompanying with it.

Fig. (3.a-d) show the effect of variation of cylinder rotation speeds on the drag coefficient (C_D) with vehicle speed ($U\infty$) equal to 90 km/h. The cases also classified according to diameter size. For the cases of D=10, 20 cm, it can be seen that the drag coefficient (C_D) increases along distance as the rotation speed increases, but in the other cases of D=30, 40 cm they are started to decrease after the rotation speed (ω) became 3000 r.p.m. This behavior is due to diameter size and the high vehicle speed ($U\infty$) velocity. For small cylinder diameter the momentum injected of the flow is small and will not create enough streamwise vortices to help the flow to cling closely to the surface which has a reverse influence on the flow.

Fig. (4.a-d) show the effect of diameter sizes on the drag coefficient (C_D) with vehicle speed of ($U\infty$) equal to 120 km/h. For the cases of ω=1000, 2000 r.p.m the figures showed a little reduction in the drag coefficient, while the case of case of ω=3000 r.p.m showed a significant reduction in the drag coefficient, Furthermore for the cases of ω =4000, 5000 r.p.m it can be seen a huge reduction in the drag coefficient. The amount of reduction depends on the diameter size, as shown in the figures and the amount of reduction increases by increasing the diameter. This is due to the significant amount of injected flow, and thus the streamwise vortices significantly increases.

Fig. (5) show the predicted distribution of velocity field vector over the surface with and without rotation, ω=0, 3000, 5000 r.p.m for each vehicle speed, $U\infty$= 90 to demonstrate the influence of rotation. It can be seen that at W=0 there is no vortices, but as the rotation starts, the effect of streamwise vortices appears and perform a significantly influence on the flow field.

CONCLUSIONS

For the case of vehicle speed ($U\infty$) equal to (40km/h), the maximum reduction in the drag coefficient obtained by using a rotation speed (ω) equal to (5000) r.p.m and a diameter equal to (40) cm. For the case of vehicle speed ($U\infty$) equal to (60km/h), the maximum reduction in the drag coefficient obtained by using a rotation speed (ω) equal to (5000) r.p.m and a diameter equal to (40) cm. For the case of vehicle speed ($U\infty$) equal to (90km/h), the maximum reduction in the drag

coefficient obtained by using a rotation speed (ω) equal to (5000) r.p.m and a diameter equal to (40) cm. For the case of vehicle speed ($U\infty$) equal to (120km/h), the maximum reduction in the drag coefficient obtained by using a rotation speed (ω) equal to (5000) r.p.m and a diameter equal to (40) cm.

Using a rotating cylinder creates stream vortices and this helps in attachment of the flow to the wall and hence delaying the separation of boundary layer separation.

REFERENCES

- Awbi, H.H. "*Ventilation of Building*", Department of Construction Management and Engineering, University of Reading, London (1991).
- Robert M.Clarke *"Truck Manufacturers Program to Reduce Aerodynamic Drag "*, Tam, Truck Manufacturers Association, April (2006).
- Robert W. Fox, Alan T. McDonald "*Introduction to Fluid Mechanics*" Second Edition, by John Wiley & Sons, Inc. (1973, 1978).
- Robonson S.E. and Ahmed, N.A. *"Drag Reduction on Bluff Bodies using a Rotating Device"* 15th Australasian Fluid Mechanics Conference, University of Sydney,(2004).
- Rose C.McCallen, Larry J.Dechant, and David Pointer W. *"DOS's Effort to Reduce Truck Aerodynamic Drag – Joint Experiments and Computations Lead to Smart Design "*34th AIAA Fluid Dynamics Conference and Exhibit, Portland, or, United States, June 28, 2004 through July 1, (2004).
- Salam H. Hussain*"Numerical investigation of Airfoil Flow Control by Means of Rotating Cylinder ",* PhD. Thesis, Mechanical Engineering Department, University of Baghdad, April (2005).
- Fayadh, and M. Abed Al-Dulaimy, R. Cousin " A CFD *Assessment to Transonic Flow Around a RAE-2822 Airfoil",* Research Reports from Guest Scientists in the Faculties 07 and 09 in the Academic year (2004/2005) Issn 1612 – 9040.
- Johan Hoffman" *Computational Study of the Effect of Rotation in a Model of the Turbulent Flow Due to a Cylinder Rolling"*,(Turbulent flow past a rolling cylinder),School of Computer Science and Communication, KTH,SE–10044 Stockholm, Sweden 1st June(2007).
- Patankar S.V. "*Numerical Heat Transfer and Fluid Flow*", Hemisphere Publishing Corporation, Taylor & Francis Group, (1980).
- Singh S. N., Rai L, Puri P. and Bhatnagar A. "*The Effect of Moving Surface On The Aerodynamic Drag of Road Vehicles",* Proc.Imeche .Vol.219 Part D: J. Automobile Engineering, (2005).
- Solberg T., and Eidsvik, K. J. *"Flow Over a Cylinder at a Plane Boundary-a Model Based Upon (k-ε) Turbulence"*, ASME Journal Vol. 111, December (1989).
- Versteeg, H.K., and Malalasekera, W. "*An Introduction to Computational Fluid Dynamics-The finite volume method*", Longman group Ltd.,(1995).

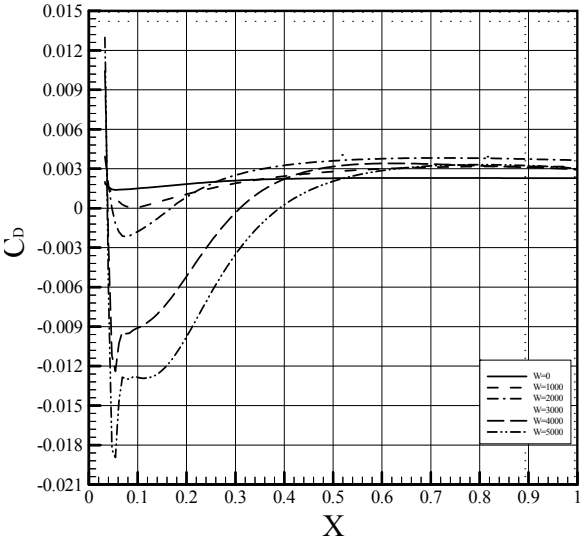

(2.a) D=10cm.

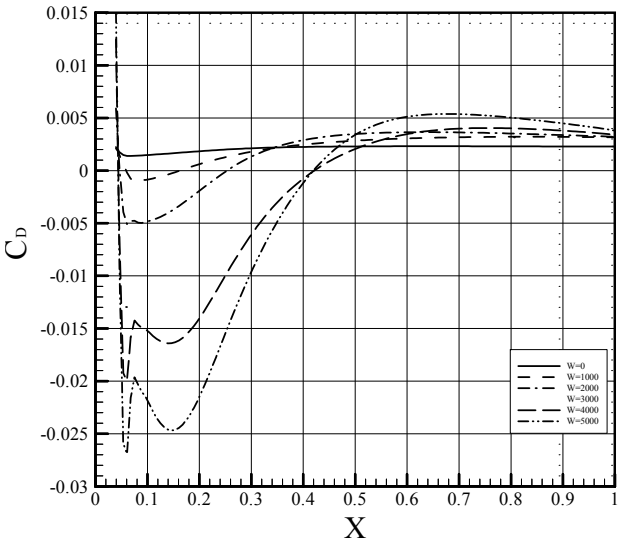

(2.b) D=20cm.

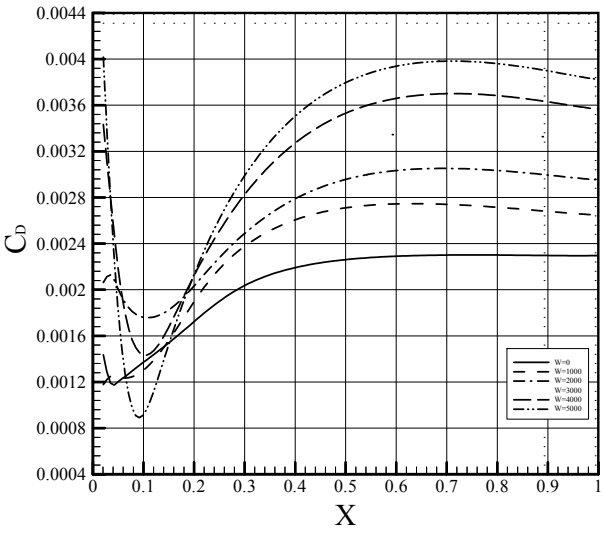

(2.c) D=30cm.

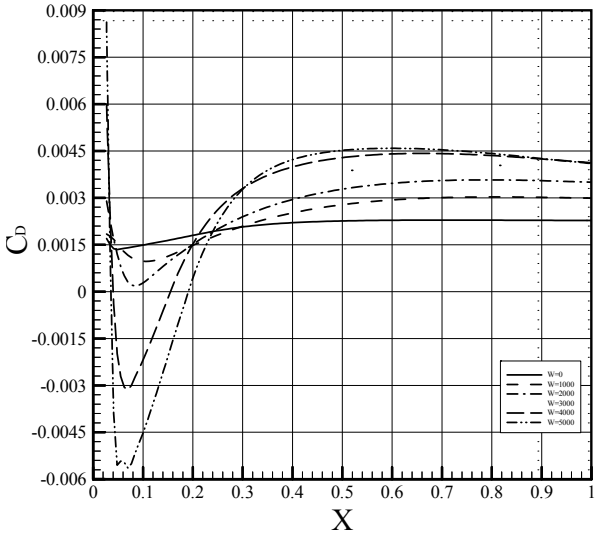

(2.d) D=40cm.

Figure. (2) Effect of cylinder rotation on drag coefficient, for vehicle speed U∞=60 km/h.

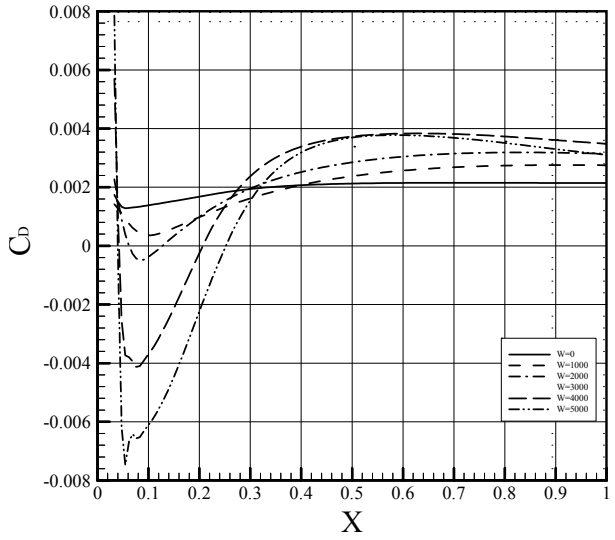

(3.a) D=10cm.

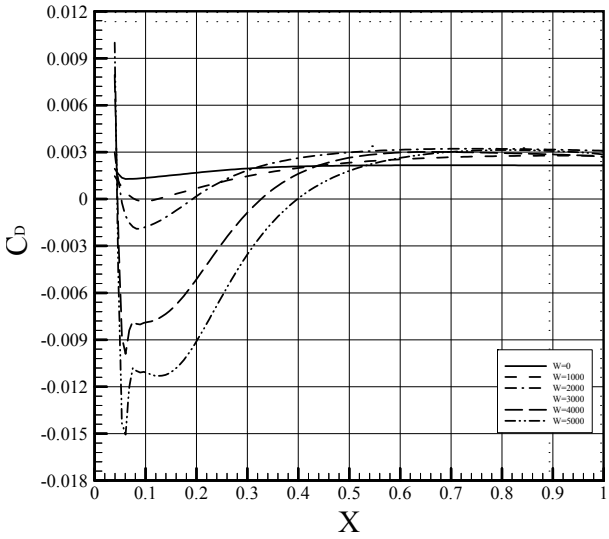

(3.b) D=20cm.

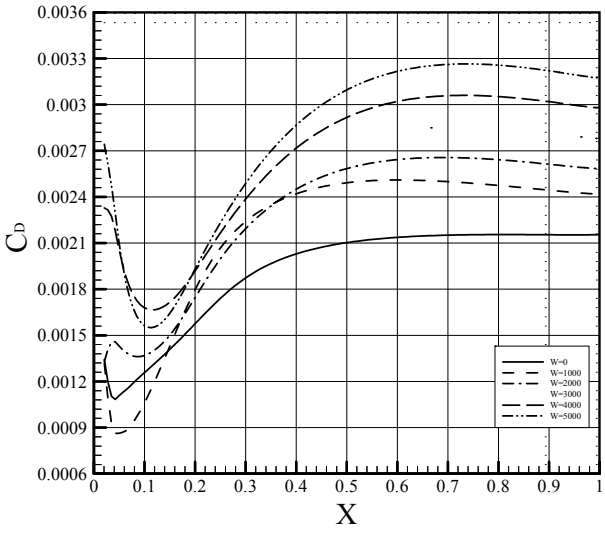

(3.c) D=30cm.

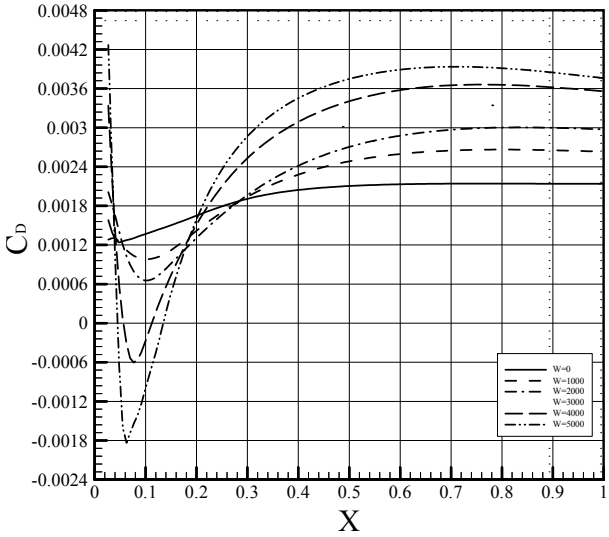

(3.d) D=40cm.

Figure. (3) Effect of cylinder rotation on drag coefficient, for vehicle speed U∞=90 km/h.

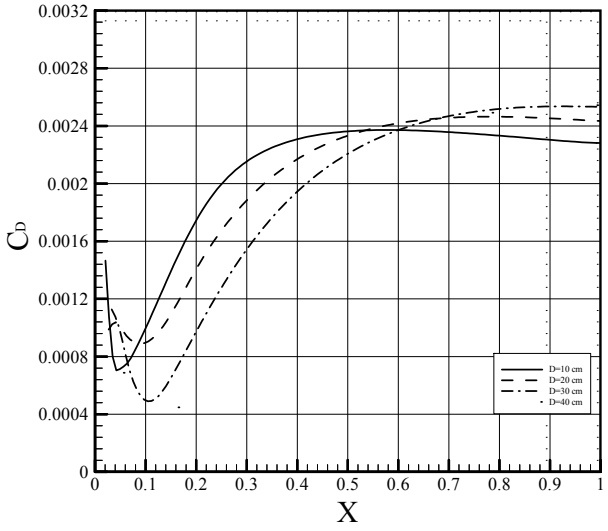

(4.a) ω=1000 r.p.m.

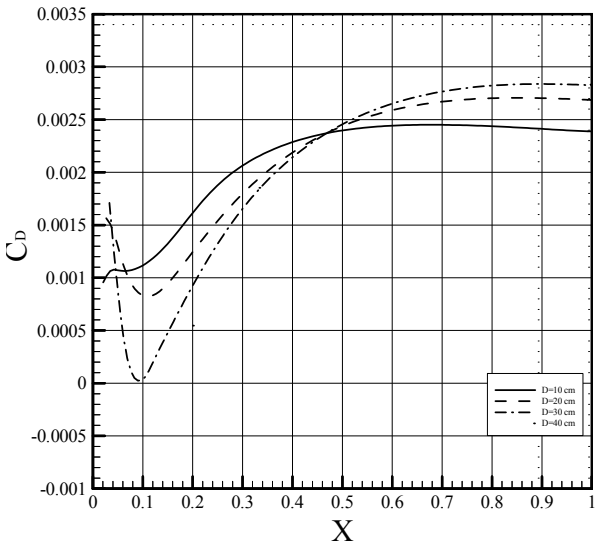

(4.b) ω=2000 r.p.m.

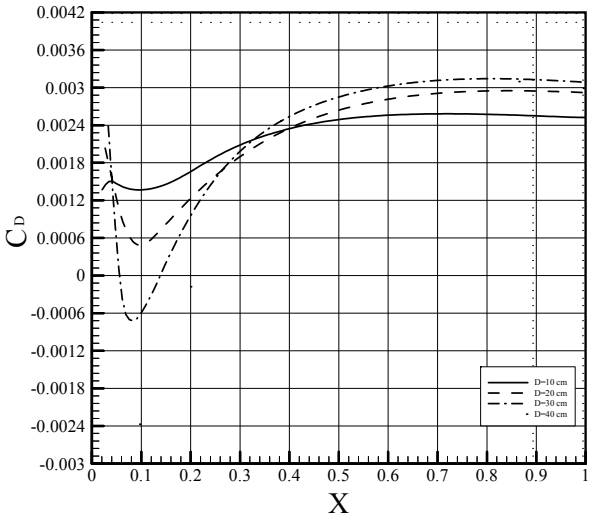

(4.c) ω=3000 r.p.m.

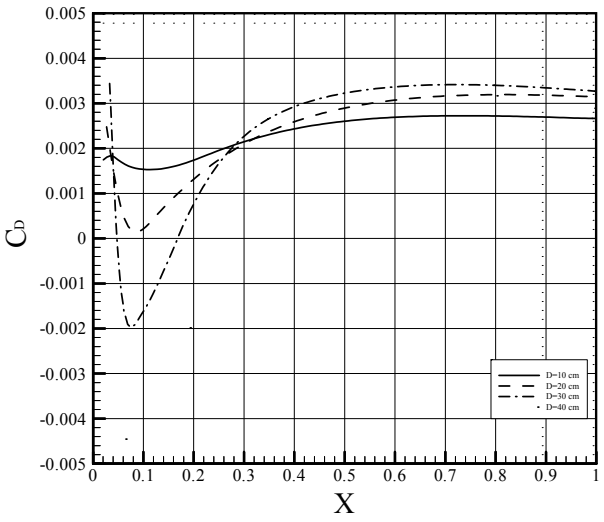

(4.d) ω=4000 r.p.

Figure. (4.a-d) Effect of cylinder diameter on drag coefficient, for vehicle speed U∞=120 km/h.

U=90 Km/h
D=40 Cm
W=0 r.p.m

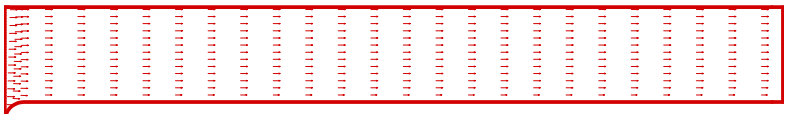

U=90 Km/h
D=40 Cm
W=3000 r.p.m

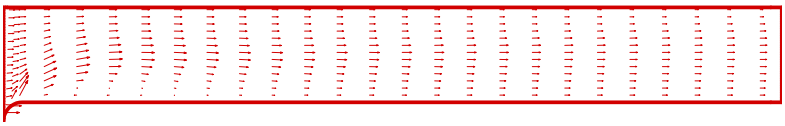

U=90 Km/h
D=40 Cm
W=5000 r.p.m

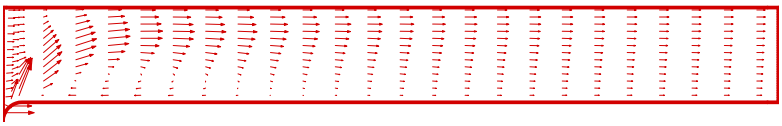

Fig. (5) Velocity field vectors over upper surface at different values of ω for vehicle speed U∞=90 km/h and D=40 cm.

NOMECLATUR

A= Convection- diffusion coefficient (kg/s)
$C_{D=}$ *coefficient of skin friction drag*
$C\mu, C_{1\varepsilon}, C_{2\varepsilon}$ *= Constants in turbulence model*
D= Diffusion term (kg/s)
F= Convection term (kg/s)
P= Pressure (Pa)
Pe= Peclet number (Pe=Re. Pr)
Re= Reynolds number ($\mathrm{Re} = \rho UL/\mu$*)*
$U\infty$ *= Relative Free stream velocity (m/s)*
U, V= Mean velocity components in x,y directions (m/s)
X, Y= Cartesian coordinates (m)
S_Φ*= Source term*
ω*= Rotational speed (r.p.m)*
Γ*= Diffusion coefficient*
ε*= Dissipation rate of turbulent kinetic*
μ*= Laminar viscosity (*k_g*/m.s)*
μ_t*= Turbulent or eddy viscosity (*k_g*/m.s)*
μ_e*= Effective eddy viscosity (*k_g*/m.s)*
ρ*= Density (*k_g/m^3*)*
λ *= Thermal conductivity (W/m.k)*
ϕ*= Dependent variable*
υ *= Kinematic viscosity (*m^2/s*)*
υ_t*= Turbulent kinematic viscosity (*m^2/s*)*
$\sigma_K, \sigma_\varepsilon$*= Constants for the K-*$\varepsilon$ *model*
σ*= Laminar Prandtl number (*$\sigma = \mu c_p/\lambda$*)*
σ_t*= Turbulent Prandtl number (*$\sigma_t = \mu_t c_p/\lambda$*)*

ABBREVIATIONS

CFD= Computational Fluid Dynamics
FVM= Finite Volume Method
SIMPLE= Semi-Implicit Method for Pressure Linked Equations
TDMA= Tri -Diagonal Matrix Algorithm